Ferroelectrics, 339:209–218, 2006

ISSN: 0015-0193 print / 1563-5112 online
DOI: 10.1080/00150190600740192

Taylor & Francis
Taylor & Francis Group

Synchrotron Radiation Study of Structural Tendencies in Aurivillius Ceramics

L. FUENTES,[1,*] J. F. FERNANDEZ,[2] MA. E. FUENTES,[3]
L. LASCANO,[4] M. E. VILLAFUERTE,[5] MA. E. MONTERO,[1]
R. OLIVERA,[1] A. MEHTA,[6] AND T. JARDIEL[2]

[1]Centro de Investigación en Materiales Avanzados, Chih., México
[2]Instituto de Cerámica y Vidrio, Arganda del Rey, España
[3]Universidad Autónoma de Chihuahua, Chih., México
[4]Escuela Politécnica Nacional, Quito, Ecuador
[5]Universidad Nacional Autonónoma de México, México
[6]Stanford Synchrotron Radiation Laboratory, Stanford, USA

A review of structural tendencies, as observed in several synchrotron radiation diffraction studies of Aurivillius phases, is presented. The role of powder synchrotron radiation is analyzed. Investigated phases belong to Aurivillius families with n *from 3 to 6, with partial substitution of small Ti cations and of large Bi cations. Representative formulas are:* $Bi_4\ Ti_{3-x}W_xO_{12}$, $Bi_{n+1}Ti_3Fe_{n-3}O_{3n+3}$ *and* $(Ba, Pb)_2\ Bi_4\ Ti_5\ O_{18}$. *Observed general behavior shows a tendency to increase disorder with increasing chemical complexity. The structure-polarization relationship in* $Ba_2Bi_4Ti_5O_{18}$ *is investigated and a paradox between published results is highlighted. Synchrotron radiation results tend to confirm Lightfoots's conclusions, suggesting electric polarization along the* z *axis.*

Keywords Synchrotron radiation; Aurivillius; crystal structure

Introduction

So-called *Aurivillius* ceramics show interesting ferroic characteristics. The crystal structure of the mentioned phases is formed by n ($n = 1, 2, 3, \ldots$) layers of perovskite octahedra, sandwiched between bismuth oxide layers.

Structure-macroscopic properties relationships in Aurivillius ceramics have been resumed in [1]. The physical basis for discussing this topic is given by the Neumann's Principle: *Any macroscopic property's point group contains the structural point group as a subgroup.* One important (and sometimes forgotten) aspect of this Principle is the fact that different space groups, associated with the same point group, show no differences in their structure-macroscopic properties symmetry relationships. The well-known rule that prohibits centro-symmetrical crystals to be piezo- or ferroelectric is derived from the Neumann's Principle. Another corollary, not always taken into account, is presented with the aid of Figs. 1 and 2. If a polarized system shows a mirror-symmetry plane, then the

Paper originally presented at IMF-11, Iguassu Falls, Brazil, September 5–9, 2005; received for publication January 26, 2006.
*Corresponding author. E-mail: luis.fuentes@cimari.edu.mx

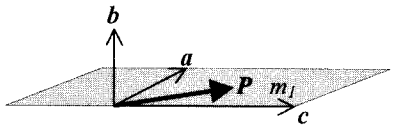

Figure 1. Polarization in monoclinic point group C_s = m. The electric dipole is parallel to the symmetry plane m_1.

electric dipole vector must be contained in the symmetry plane. For crystals belonging to monoclinic point group $C_s = m$, the permanent electric dipole may point along any direction within the structural mirror plane (Fig. 1). For point group $C_{2v} = 2\,mm$, the electric dipole necessarily points along the intersection of the two mirror planes, i.e. along the two-fold axis (Fig. 2). There exist 22 orthorhombic space groups that are generated from point group C_{2v}. For all of them, the existence of permanent electric dipole components perpendicular to the two-fold symmetry axis is forbidden.

Powder diffractometry projects the three dimensional reciprocal lattice into a one dimensional reciprocal space. Such a projection causes partial [total] overlap of peaks with similar [equal] lattice spacings. Peak overlap leads to loss of information and so single-crystal methods are better for the determination of electron-density distributions and other structural data. On the other hand, the one-dimensional nature of powder diffraction practically eliminates the influence of zero-shift and other systematic errors in the detection of very small lattice spacing *differences*. So, powder peak overlap becomes a useful tool in investigations of subtle symmetry break-downs, which are often missed in single crystal measurements. The mentioned advantage of powder diffraction grows up when we include the consideration of high-resolution (synchrotron and neutron) present-day powder diffractometers. As an example, consider the discovery of a monoclinic phase in the PZT system [2]. It was a surprising finding. The measured lattice parameters were a = 5.717 Å, b = 5.703 Å, c = 4.143 Å, $\beta = 90.53°$. The experiment was a synchrotron high-resolution *powder* diffraction investigation.

The preceding discussion supports the convenience of careful synchrotron powder diffraction experiments focused on the detection of subtle crystal symmetry changes in Aurivillius phases. Mentioned symmetry investigations may contribute significant elements to our understanding of the structure-properties relationships in the Aurivillius' materials family.

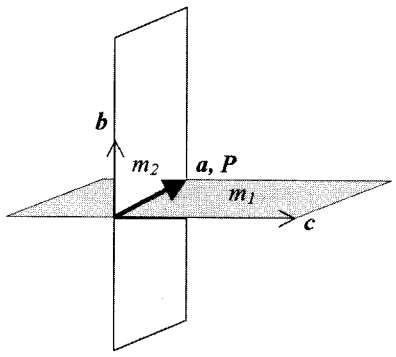

Figure 2. Polarization in orthorhombic point group C_{2v}= 2 mm. The electric dipole belongs to the intersection of symmetry planes m_1 and m_2.

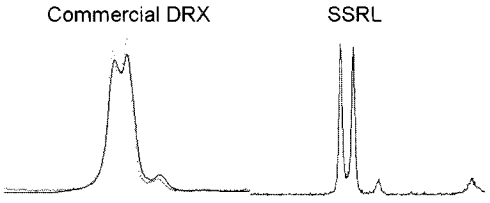

Figure 3. Comparison between resolutions at a conventional x-ray diffractometer and the beamline 2-1 powder diffractometer at SSRL. (See Color Plate XII).

Experiments and Results

The experimental basis for the present investigation is the x-ray powder diffractometer located at beamline 2-1 of the Stanford Synchrotron Radiation Laboratory (SSRL) [3]. For comparison with conventional diffractometry, consider Fig. 3. The plots refer to the (2, 0, 0/0, 2, 0) doublet from the Aurivillius compound $Bi_5FeTi_3O_{15}$. Measurements were done in a commercial equipment and in the SSRL powder diffractometer. The considered doublet is an important characteristic of any Aurivillius diffraction pattern. It clearly reveals the difference between *a* and *b* lattice parameters, so it is an indicator of a *tetragonal* → *orthorhombic* symmetry break-down. When available, the (4, 0, 0 / 0, 4, 0) doublet represents a better indicator. Unfortunately, the last mentioned doublet frequently appears superposed with other reflections.

We now present the variations detected in the diffraction patterns of some Aurivillius phases as dependent on composition changes and comment on results' structural interpretation. Our first study refers to iron-containing multiferroics. The crystal structure of 4-layered $Bi_5FeTi_3O_{15}$ has been reported by some researchers [4, 5], including the authors of the present report [6]. Room temperature structure is orthorhombic, space group $A2_1am$ [4] or F2 mm [5, 6]. Lattice parameters (Å) are a = 5.4759(2), b = 5.4420(2) and c = 41.157(1). Figure 4 shows the SSRL-XRD pattern of this phase and Fig. 5 represents the structure.

The 5-layered member of this family is $Bi_6Fe_2Ti_3O_{18}$. The structure and stability of this phase are being studied at present. The occurrence of Fe^{3+} cations in the B perovskite sites

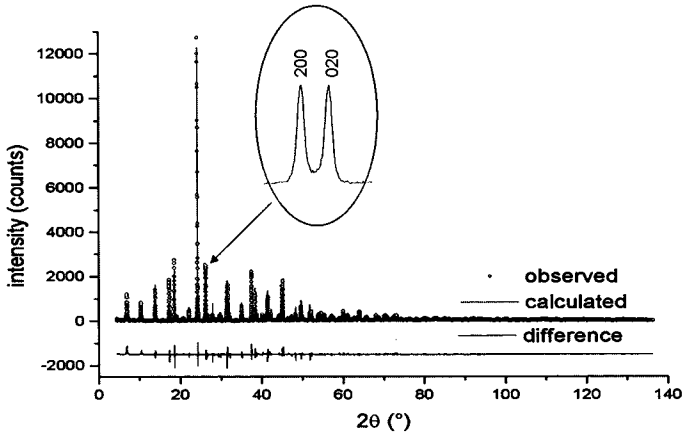

Figure 4. $Bi_5Ti_3FeO_{15}$—Diffraction investigation at SSRL.

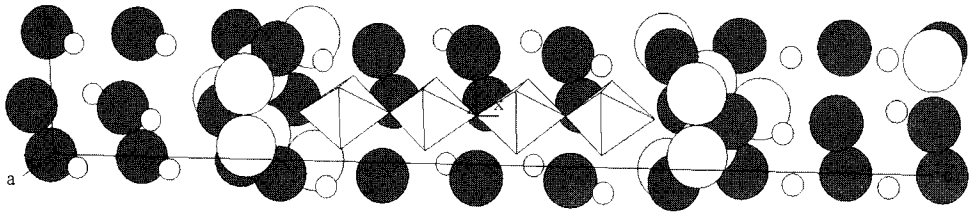

Figure 5. The crystal structure of $Bi_5Ti_3FeO_{15}$. Spheres: large white → O; small white → Ti; large gray → Bi. O atoms at the corners of Ti-coordination octahedra omitted.

increases the elastic tension between the bismuth oxide layers and the perovskite domain of the unit cell (atomic radiuses (Å): Fe^{3+} → 0.67; Ti^{4+} → 0.64). Figure 6 characterizes the event that occurs in relation with the (2, 0, 0/0, 2, 0) doublet. "BTF" denotes the 4-layered compound and "BTF2" refers to the 5-layered one. Doublets have been shifted to impose coincidence of the lower-angle (2, 0, 0) peaks. Refined lattice parameters (Å) are a = 5.4966(2); b = 5.4656(2) and c = 49.340(1). The experiment indicates that the cell grows (also) parallel to the bismuth oxide layers and that the difference between [a, b] parameters slightly decreases as the number of layers increases.

Our second case refers to the substitution of Ti^{4+} cations by small quantities of W^{6+} (atomic radius: 0.65) in BIT = $Bi_4Ti_3O_{12}$. The objective of doping is conductivity control.

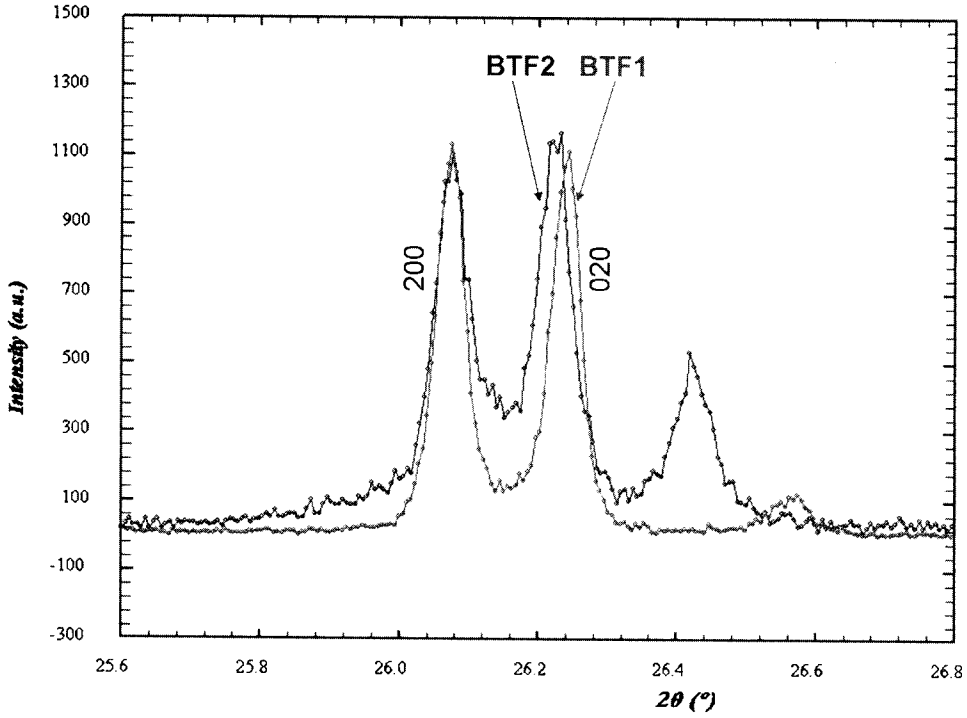

Figure 6. Splitting of the (2, 0, 0/0, 2, 0) diffraction peaks as dependent on the number of perovskite layers. Fe-Ti Aurivillius phases. (See Color Plate XIII).

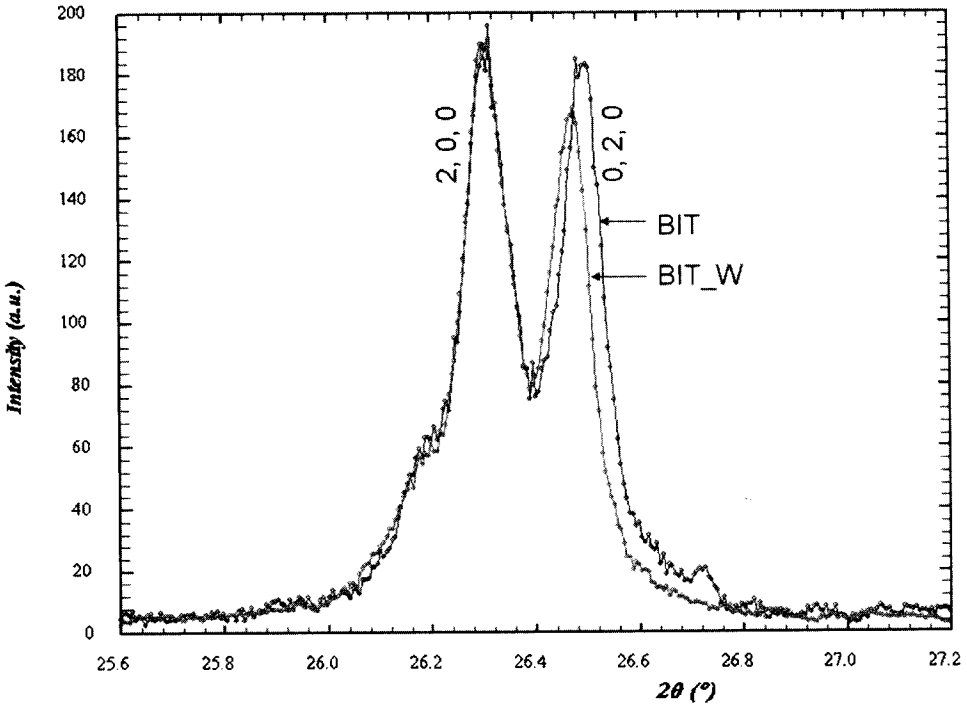

Figure 7. Effect of W-doping on the fine structure of $Bi_4Ti_3O_{12}$. (See Color Plate XIV).

Figure 7 shows the tiny-but-detectable diffraction effect of 5% W substitution on the Ti sites.

The comparison between *doped* and *non-doped* lattice parameters (Å) is as follows.

BIT	BIT_W(W → Ti @ 5at %)
5.44826 ± 0.00016	5.44583 ± 0.00013
5.41083 ± 0.00015	5.41252 ± 0.00012
32.84081 ± 0.00090	32.85387 ± 0.00073

$$(a-b)_{BIT} = (a-b)_{BITW} + 0.004 \text{ Å}$$

Figure 8 focuses on a case of large cations' substitution. We consider the Pb-containing Aurivillius series with $n = 4$, 5 and 6 perovskites layers. The formulas are PBiT = $PbBi_4Ti_4O_{15}$, P2BiT = $Pb_2Bi_4Ti_5O_{18}$ and P3BiT = $Pb_3Bi_4Ti_6O_{21}$. One important question here is the distribution of Pb^{2+} cations among the perovskite A sites and the bismuth oxide layers. The electronic structure of Pb^{2+} cations is similar to that of Bi^{2+}: both have $(ns)^2$ valence electron configuration. The PBiT series exhibits the favorable condition that the (4, 0, 0/0, 4, 0) doublets appear clean of interference. Figure 8 describes the comparison among the mentioned doublets in the considered phases. The results are remarkable: a − b difference clearly diminishes as the number of layers increases. P1BiT and P2BiT are obviously orthorhombic, but P3BiT reveals itself as tetragonal. A detailed discussion of structural aspects of the PBiT family is exposed in IMF-11 [7].

Our final section discusses in detail Aurivillius phases containing Ba. We analyze the particular relationship between the permanent polarization of the ($n = 5$) compound $Ba_2Bi_4Ti_5O_{18}$ (B2BiT) and its crystallographic structure.

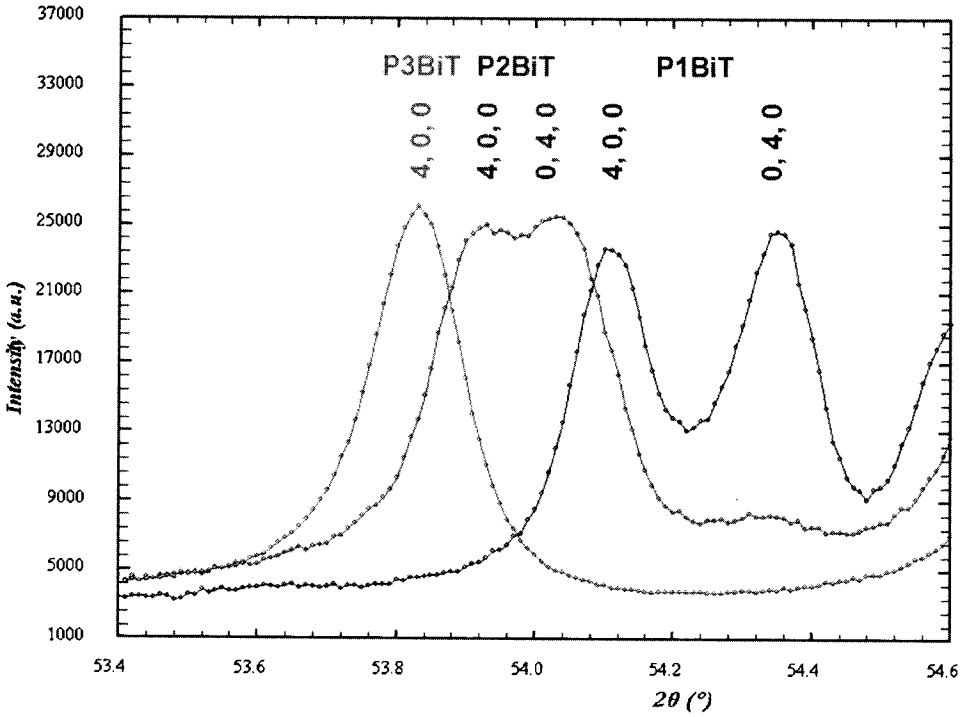

Figure 8. Investigation of the (4, 0, 0/0, 4, 0) splitting in the PBiT series. (See Color Plate XV).

In an interesting paper, Irie and collaborators [8] report the measurement of the ferroelectric hysteresis loops corresponding to different orientations of a $Ba_2Bi_4Ti_5O_{18}$ single-crystal. Regarding the room temperature remanent polarizations along the x and z axes, they find the following values: $P_x = 120$ mC/m^2; $P_z = 8.5$ mC/m^2. The z axis points perpendicular to the Bi-oxide layers, while the x axis is parallel to these layers. Irie et al. also investigated the crystal symmetry of the considered compound. From room temperature x-ray diffraction data they propose the orthorhombic space group *B2ab*.

More recently, based on high-resolution neutron diffraction data, Lightfoot and coworkers [9] state that—at room temperature—the crystal symmetry of $Ba_2Bi_4Ti_5O_{18}$ is tetragonal, with space group *I4mm*. These authors suggest a non-previously proposed polarization scheme, with ionic displacements only along the z axis.

These two groups' results are in contradiction with each other. The paradox goes deeper than differences in the proposed space groups. None of the mentioned symmetries is compatible with the single-crystal polarization reported in [8].

In an attempt to clarify the eventual break-down of tetragonal symmetry in $Ba_2Bi_4Ti_5O_{18}$, a synchrotron radiation study of this phase was performed. Polycrystalline $Ba_2Bi_4Ti_5O_{18}$ was prepared by a conventional ceramic procedure. Stoichiometric quantities of Bi_2O_3 (Riedel-de Haen, 99.5%), TiO_2 (Merck, >99%) and BaTiO3 (ICV-CSIC [4]) were homogenised for 3 hours in a ZrO_2 planetary mill. After drying and sieving, the intimately mixed materials were heated in air at 1100°C for 2 hours. The formation of a single-phase oxide was confirmed by conventional powder XRD.

The synchrotron radiation diffraction pattern was cautiously examined in the vicinity of $2\theta \approx 26.2°$. In the *F2mm* space group description, this is the angular position (for 10 KeV x-rays) of the (2, 0, 0/0, 2, 0) doublet splitting. In the present investigation, to highlight the

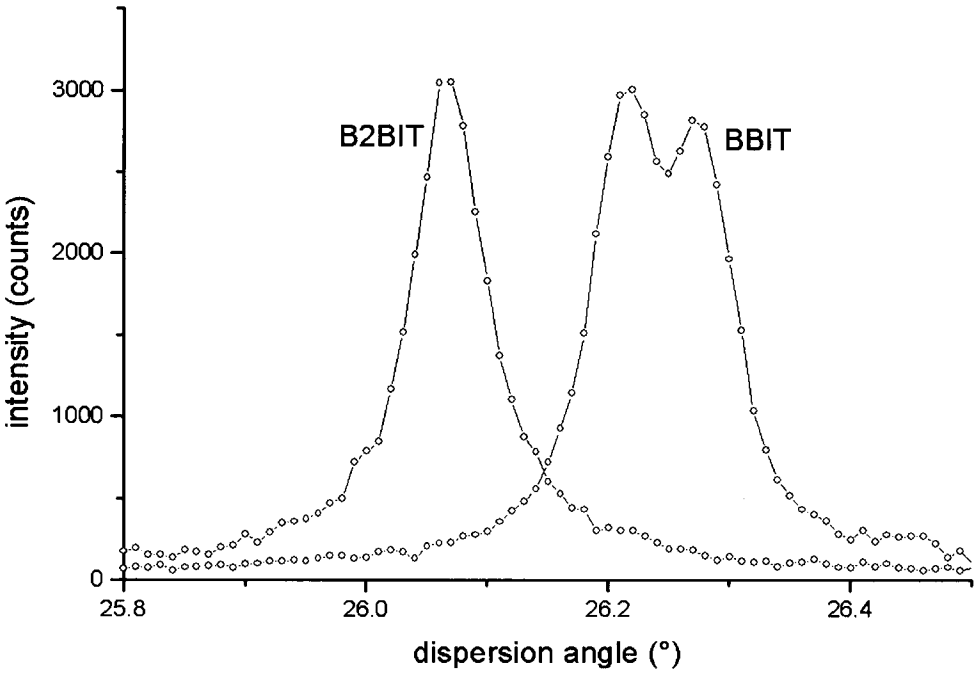

Figure 9. Comparison between (2, 0, 0/0, 2, 0) doublets (F2mm representation). $Ba_2Bi_4Ti_5O_{18}$ (B2BIT) and $BaBi_4Ti_4O_{15}$ (BBIT).

detection (or not) of the considered splitting, a comparison with the experimental pattern from $BaBi_4Ti_4O_{15}$ ($n = 4$, BBiT [10]) was performed. Figure 9 shows in magnification the mentioned comparison. Both diffraction experiments were performed under identical conditions. The difference is striking. Synchrotron x-ray diffraction pattern from B2BiT does not show tetragonal symmetry break-down.

Rietveld refinement was performed with program Fullprof [11]. Starting space group followed Aurivillius' choice *I4/mmm* [12]. Semi-quantitative agreement was obtained. To further proceed, the constraint of centro-symmetrical symmetry was released. Lightfoot et al. suggestion of *I4mm* space group was tested and a final satisfactory convergence was reached with this space group. Figure 10 shows the Rietveld refinement plots.

Table 1 contains the results of the performed structural analysis. Numbers in parentheses are standard deviations. The absence of parentheses means that the considered quantity remained fixed during the refinement. Highly symmetric oxygen sites were taken as reference coordinates. Titanium cations' temperature factors did not show stability during refinement. Their standard deviations were not significantly lower than their values or variations. Consequently these parameters were fixed.

Figure 11 represents the B2BIT calculated structure. Figure 12 shows selected interatomic distances in the asymmetric unit. The presented figures show some longitudinal distortion of the perovskite octahedra along the z axis, small departures from inversion symmetry and the possibility of electric dipole component P_z.

Substitution of Bi by Ba in the oxide layer is unexpected. Ba^{2+} does not show the lone pair activity that provides accommodation in the given unsymmetrical environment. On the other hand, Rietveld refinement converged to the reported stable values when Bi/Ba

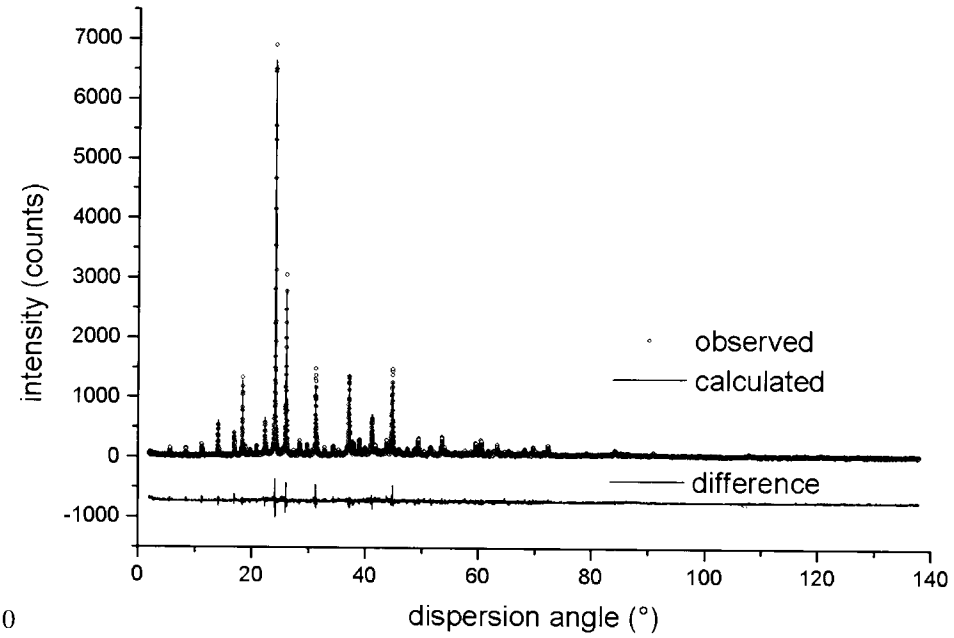

10

Figure 10. Observed and calculated diffraction patterns for $Ba_2Bi_4Ti_5O_{18}$. 10 KeV x-rays from beamline 2-1 in Stanford Synchrotron Radiation Laboratory.

occupation factors were released in perovskite A-sites [Bi/Ba(1),... Bi/Ba(4)] as well as in the oxide layers [Bi/Ba(x1), Bi/Ba(x2)]. References [13, 14] also report results of this kind. Final clarification of the occupancy question will maybe come from a careful x-ray absorption spectroscopy (XAS) investigation [15].

Now the B2BiT paradox is considered.

A first observation is required in relation to the internal consistency of Irie's results. The space group proposed in the mentioned work, namely *B2ab* (associated with point group *2mm*), is incompatible with the existence of two components in the polarization vector, as reported in Irie's polarization curves (Fig. 9 of ref. [8]). According to polarization results, B2BiT could not be orthorhombic; maximum possible symmetry would be monoclinic.

But, neutron [9] and synchrotron (present investigation) diffraction results indicate that B2BiT is tetragonal.

In conclusion, polarization and diffraction results don't fit. Something has gone out of control. Some possible explanations could be suggested:

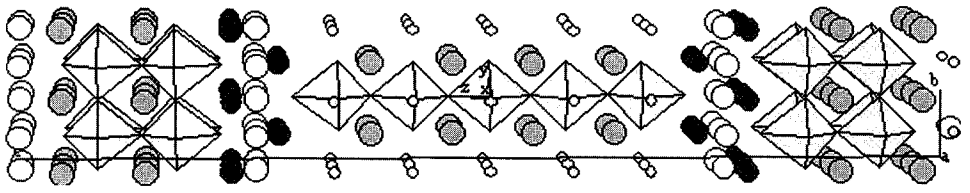

Figure 11. The crystal structure of $Ba_2Bi_4Ti_5O_{18}$. $2 \cdot 2 \cdot 1 = 4$ unit cells are shown. Large spheres: white → O; gray → Ba/Bi. Small spheres and inside octahedral → Ti. Octahedra corners → O.

Table 1
Atomic parameters for $Ba_2Bi_4Ti_5O_{18}$

Atom	x	y	z(σ_z)	B(σ_B)	Occupancy(σ_{occ})
Bi/Ba(x1)	0.00000	0.00000	0.7769(8)	1.12(7)	0.87(1)/0.13(1)
Bi/Ba(x2)	0.00000	0.00000	0.2271(8)	1.12(7)	0.87(1)/0.13(1)
Bi/Ba(1)	0.00000	0.00000	0.9551(8)	3.08(7)	0.57(1)/0.43(1)
Bi/Ba(2)	0.00000	0.00000	0.0408(8)	3.08(7)	0.57(1)/0.43(1)
Bi/Ba(3)	0.00000	0.00000	0.8684(8)	3.08(7)	0.57(1)/0.43(1)
Bi/Ba(4)	0.00000	0.00000	0.1287(8)	3.08(7)	0.57(1)/0.43(1)
Ti1	0.00000	0.00000	0.502(1)	0.10	1.000
Ti2	0.00000	0.00000	0.5858(8)	0.10	1.000
Ti3	0.00000	0.00000	0.6691(8)	0.10	1.000
Ti4	0.00000	0.00000	0.3315(8)	0.10	1.000
Ti5	0.00000	0.00000	0.4146(8)	0.10	1.000
O(x1)	0.00000	0.50000	0.0000	2.9(2)	1.000
O(x2)	0.00000	0.50000	0.2500	2.9(2)	1.000
O1	0.00000	0.00000	0.5451(8)	2.9(2)	1.000
O2	0.00000	0.00000	0.6283(8)	2.9(2)	1.000
O3	0.00000	0.00000	0.7125(8)	2.9(2)	1.000
O4	0.00000	0.00000	0.2883(8)	2.9(2)	1.000
O5	0.00000	0.00000	0.3723(8)	2.9(2)	1.000
O6	0.00000	0.00000	0.4554(8)	2.9(2)	2.000
O7	0.00000	0.50000	0.0815	2.9(2)	1.000
O8	0.00000	0.50000	0.1630	2.9(2)	1.000
O9	0.00000	0.50000	0.8370	2.9(2)	1.000
O10	0.00000	0.50000	0.9185	2.9(2)	1.000

Space group: *I4mm*.
Cell parameters (Å): a = b = 3.8874 (1); c = 50.369 (2).
Reliability factors: $R_{Bragg} = 9.03$; $R_p = 13.1$; $\chi^2 = 2.67$.

- Insufficient resolution in the diffraction experiments.
- Human errors, for example in crystal orientation.
- Differences in sample preparation may have lead to different degrees of preservation of a metastable high-temperature phase.
- Short-range symmetry break-downs. A plausible cause for this effect may be the existence of oxygen defects [16]. Consideration of local disorders, not detected by "average structure" diffraction methods, could lead to a solution of the investigated paradox.

Further work, possibly by XAS [15][17], is required to solve the stated problem.

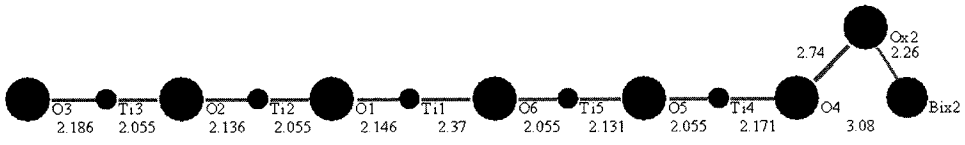

Figure 12. Representative interatomic distances (Å) in $Ba_2Bi_4Ti_5O_{18}$ asymmetric unit.

Regarding general tendencies observed, as chemical composition of Aurivillius phases becomes more complex, orthorhombic splitting tends to decrease; disorder and symmetry tend to increase.

Acknowledgments

Portions of this research were carried out at the Stanford Synchrotron Radiation Laboratory, a national user facility operated by Stanford University on behalf of the U.S. Department of Energy, Office of Basic Energy Sciences. Special thanks to the Materials Corridor Initiative and to Prof. R. Chianelli. Support from CONACYT-Mexico (Project CIAM 42361: Multiferroic Materials) and from Program CYTED (Sub-Program VIII, Project VIII.13: Electroceramic Materials) is gratefully acknowledged.

References

1. L. Fuentes, M. E. Fuentes, and H. Camacho, Aurivillius ceramics: Focus on symmetry. *Ferroelectrics* **274**, 317–322 (2002).
2. Noheda, Cox, and Shirane, *Appl. Phys. Lett.* **74**, 2059 (1999).
3. http://smb.slac.stanford.edu/powder/
4. C. H. Hervoches, A. Snedden, R. Riggs, S. H. Kilcoyne, P. Manuel, and P. Lightfoot, Structural behavior of the four-layer Aurivillius-phase ferroelectrics Sr $Bi_4Ti_4O_{15}$ and $Bi_5Ti_3FeO_{15}$. *J. Solid State Chemistry* **164**, 280–291 (2002).
5. F. Kubel and H. Schmid, X-ray room temperature structure from single crystal data, powder diffraction measurements and optical studies of the Aurivillius phase $Bi_5(Ti_3Fe)O_{15}$. *Ferroelectrics* **129**, 101–112 (1992).
6. M. Garcia-Guaderrama, L. Fuentes, M. E. Montero-Cabrera, A. Marquez-Lucero, and M. E. Villafuerte-Castrejon. Molten salt synthesis and crystal structure of $Bi_5Ti_3FeO_{15}$. *Integrated Ferroelectrics* **71**, 233–239 (2005).
7. Ma. E. Villafuerte-Castrejón, L. Fuentes, A. Ibarra-Palos, J. Castro, L. Bucio, and L. Fuentes-Montero, Symmetry in the lead bismuth titanium oxides. International Meeting on Ferroelectrics, Contribution IMF-18-016 (2005).
8. H. Irie, M. Miyayama, and T. Kudo, Electrical properties of a bismuth layer-structured $Ba_2Bi_4Ti_5O_{18}$ single crystal. *J. Am. Ceram. Soc.* **83**, 2699–2704 (2000).
9. P. Lightfoot, A. Snedden, S. M. Blake and K. S. Knight, Contrasting structural behavior in the Aurivillius phase ferroelectrics $Bi_4Ti_3O_{12}$, $BaBi_4Ti_4O_{15}$ and $Ba_2Bi_4Ti_5O_{18}$. *Mat. Res. Soc. Symp. Proc.* **755**, DD4.7.1-8 (2003).
10. M. E. Fuentes, A. Mehta, L. Lascano, H. Camacho, R. Chianelli, J. F. Fernández, and L. Fuentes, The crystal structure of $BaBi_4Ti_4O_{15}$. *Ferroelectrics* **269**, 159–164 (2002).
11. J. Rodriguez-Carvajal, *Physica B* **192**, 55 (1993).
12. B. Aurivillius and P. H. Fang, Ferroelectricity in the compound $Ba_2Bi_4Ti_5O_{18}$. *Physical Review A* **126**, 893–896 (1962).
13. S. M. Blake, M. J. Falconer, M. Mc.Creedy, and P. Lightfoot, Cation disorder in ferroelectric Aurivillius phases of the type $Bi_2ANb_2O_9$ (A = Ba, Sr, Ca). *J. Mater. Chem.* **7**(8), 1609–1613 (1997).
14. N. C. Hyatt, J. A. Hriljac, and T. P. Comyn, Cation disorder in $Bi_2Ln_2Ti_3O_{12}$ Aurivillius phases (Ln = La, Pr, Nd and Sm). *Materials research Bulletin* **38**, 837–846 (2003).
15. J. J. Rehr and R. C. Albers, Theoretical approaches to x-ray absorption fine structure. *Rev. Modern Phys.* **72**(3), 621–654 (2000).
16. Y. Noguchi and M. Miyayama, Defects and functions in ferroelectric memory materials. *J. Cryst. Soc. Jpn.* **46**(1), 3–8 (2004).
17. P. P. Neves, A. C. Doriguetto, V. R. Mastelaro, L. P. Lopes, Y. P. Mascarenhas, A. Michalowicz, and J. A. Eiras, XAS and XRD Structural characterization of lanthanum-modified $PbTiO_3$ ceramic materials. *J. Phys. Chem. B* **108**, 14840–14849 (2004).